Chinese Chemical Letters 33 (2022) 3492–3496

Contents lists available at ScienceDirect

Chinese Chemical Letters

journal homepage: www.elsevier.com/locate/cclet

Facile preparation of ^{177}Lu-microspheres for hepatocellular carcinoma radioisotope therapy

Manran Wu[a], Kexin Shi[a], Ruizhe Huang[a], Chunyi Liu[a], Lingling Yin[a], Weipeng Yong[a], Jing Sun[a], Guanglin Wang[a,*], Zhiyuan Zhong[b], Mingyuan Gao[a,*]

[a] State Key Laboratory of Radiation Medicine and Protection, School of Radiation Medicine and Protection & School for Radiological and Interdisciplinary Sciences (RAD-X), Collaborative Innovation Center of Radiation Medicine of Jiangsu Higher Education Institutions, Soochow University, Suzhou 215123, China
[b] Biomedical Polymers Laboratory, College of Chemistry, Chemical Engineering and Materials Science, State Key Laboratory of Radiation Medicine and Protection, Soochow University, Suzhou 215123, China

ARTICLE INFO

Article history:
Received 3 November 2021
Revised 29 December 2021
Accepted 6 January 2022
Available online 13 January 2022

Keywords:
Radioisotope
Radioactive microspheres
Hepatocellular carcinoma
SPECT/CT
Radioembolization therapy

ABSTRACT

As one of the most common cancers in the world, hepatocellular carcinoma (HCC) has become a major threat to human health. Radioembolization is a first-line option for the treatment of HCC, especially when other conventional treatments fail or there exist some relative contraindications. Herein, we developed a facile and efficient method for preparing ^{177}Lu-microspheres potentially useful for precise radioembolization therapy of HCC. The radiolabeling efficiency of ^{177}Lu-microspheres was as high as 96.8% ± 0.5%, and the radiolabeling process did not alter the morphology of the mother microspheres. The SPECT/CT studies enabled by the unique emissions of ^{177}Lu suggested that almost no ^{177}Lu ion loaded by the microspheres was released over more than 32 d *in vivo*, which led to remarkable inhibition effect on the growth of HepG2 tumors subcutaneously transplanted in mice. The current approach may thus offer promising ^{177}Lu-microspheres for clinical radioembolization of HCC.

Hepatocellular carcinoma (HCC) is one of the most common cancers in the world and poses a major threat to human health [1,2]. Current therapeutic strategies for HCC in the clinics mainly comprise surgical resection, liver transplantation, radiofrequency ablation, and transarterial embolization [3–7]. Among those strategies, transarterial embolization as an attractive treatment method, including transarterial chemoembolization and transarterial radioembolization (TARE), kills the tumor cells by blocking the hepatic artery [8–11]. TARE is a local radionuclide therapy that relies on radioactive materials, like gel, microparticles, and microspheres, to block the artery, so as to maximize the radiation dose in the tumor and minimize the damage to normal liver tissue. TARE is suitable for treating patients who suffer from unresectable liver cancer, or fail from other therapies [12–14].

Radioactive microspheres have been demonstrated to be an ideal carrier for TARE [15,16]. To date, three types of radioactive microspheres are clinically available, including ^{90}Y-labeled glass microspheres (TheraSphere), ^{90}Y-labeled resin microspheres (SIR-Spheres), and ^{166}Ho-labeled poly(L-lactic acid) (PLLA) microspheres (QuiremSpheres). However, all these types of microspheres suffer from some shortcomings. For instance, ^{90}Y-glass microspheres and ^{166}Ho-microspheres are produced by neutron activation, which not only requires a nuclear reactor but also produces simultaneously other long half-life radioisotopes unwanted. Although the production of ^{90}Y-resin microspheres does not have the above problems, the radiostability of the microspheres needs to be improved. In addition, ^{90}Y is a pure beta emitter. It is therefore not suitable for biomedical imaging, let alone the evaluation of possible leakage of the loaded ^{90}Y *in vivo* [17–21]. In order to overcome these limitations, a variety of different radioactive microspheres have been developed, such as ^{90}Y polymeric microspheres, ^{131}I polymeric microspheres, ^{188}Re-human serum albumin microspheres, and ^{188}Re polymeric microspheres [22–28]. However, ^{131}I emits high energy gamma ray (364 keV), which may cause damage to healthy organs, especially the lung. The half-life of ^{188}Re is as short as 16.9 h, which is inconvenient for delivery from the production site to the customer. Moreover, the initial injected activity of ^{188}Re has to be approximately 2.8 times higher than that of ^{90}Y to achieve a comparable dose, which requires more shielding precaution for protecting the physicians.

Apart from the carrier used in radioembolization, the other important factor that affects the therapeutic efficiency is the radionuclide. Among many radionuclides, ^{177}Lu is a very attractive

* Corresponding authors.
E-mail addresses: glwang@suda.edu.cn (G. Wang), gaomy@iccas.ac.cn (M. Gao).

https://doi.org/10.1016/j.cclet.2022.01.007
1001-8417/

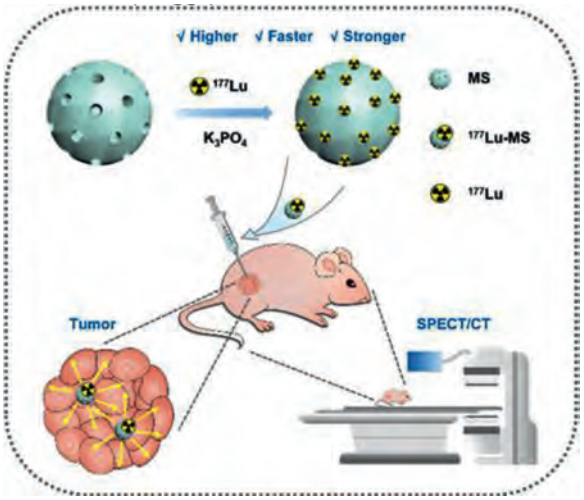

Scheme. 1. A facile preparative approach for ^{177}Lu-labeled silica microspheres (^{177}Lu-MS) for precise hepatocellular carcinoma radioisotope therapy.

one. Because it emits medium-energy beta particles (490 keV) and low-energy gamma rays (113 keV (3%), 210 keV (11%)), which provides an opportunity for observing the positioning of ^{177}Lu labeled microspheres with single-photon emission computed tomography (SPECT) imaging apart from radioisotope therapy. In addition, the proper half-life of ^{177}Lu, *i.e.*, 6.7 d, makes it suitable for transportation and clinical application [29,30]. Therefore, ^{177}Lu has been used in peptide radioligand therapy for prostate cancers and peptide receptor radionuclide therapy for neuroendocrine tumors [31–34]. More importantly, there exist several reactors in the world that can commercially supply ^{177}Lu.

In this study, we developed a facile and efficient method for preparing ^{177}Lu-microspheres by directly precipitating ^{177}Lu on commercial silica microspheres for HCC radioisotope therapy and imaging (Scheme 1). Silica microspheres are a kind of material that is easy to prepare, has a controllable morphology and good biocompatibility [35,36]. The obtained ^{177}Lu-microspheres showed both controllable specific activities and high radiostability. HepG2 subcutaneous tumor-bearing mice were used for *in vivo* biodistribution and anti-tumor inhibition evaluation. *In vivo* biodistribution monitored by *micro*SPECT indicated that ^{177}Lu-microspheres were retained in the tumor even 32 d after intratumoral injection. Most importantly, the above ^{177}Lu-microspheres presented a remarkable anti-tumor inhibition efficiency.

^{177}Lu-microspheres were prepared through a precipitation method by using silica microspheres as matrix. K_3PO_4 and KOH were used to adjust the pH of the reaction medium as the precipitation reactions of $^{177}Lu^{3+}$ are generally pH-dependent. As shown in Fig. 1A, the radiolabeling efficiency increases dramatically against pH and reaches a plateau around 96.8% ± 0.5% at pH 12. In addition, the effect of reaction time on the radiolabeling efficiency was also studied. According to the results given in Fig. 1B, the radiolabeling efficiency higher than 96% can be achieved within 1 min, nearly independent of the reaction time. The following studies suggested that the specific activity, calculated by dividing the radioactivity of ^{177}Lu by the number of microspheres, could be varied from 1 Bq/microsphere to 1×10^5 Bq/microsphere through the approach mentioned above. High specific activity is favorable for avoiding arterial stasis caused by excessive microspheres, as less number of microspheres is required for achieving the same radiation dose [37,38]. To characterize the morphology, size and size distribution of the microspheres after ^{177}Lu labeling, $^{175}LuCl_3$ was used instead of $^{177}LuCl_3$ to prepare non-radioactive microspheres (denoted as Lu-microspheres) following the same preparative procedures for ^{177}Lu-microspheres. The average size of the Lu-microspheres determined by optical microscopy is of 20.7 ± 0.7 μm and the polydisperse index is of 0.034, as shown in Fig. 1C and Fig. S1A (Supporting information). The scanning electron microscopy (SEM) image given in Fig. 1D reveals that the Lu-microspheres are perfectly spherical in shape. In comparison with the mother silica microspheres, the Lu-microspheres present nearly unchanged shape, size and size distribution, suggesting that the coprecipitation approach did not alter the morphology of the mother silica microspheres at all (Figs. S1B-D in Supporting information). The radiostability of ^{177}Lu-microspheres in saline and 10% FBS was tested and the free ^{177}Lu in saline and 10% FBS was measured to be less than 2% and 20% (Fig. 1E), respectively, indicating that ^{177}Lu-microspheres are very stable for further *in vitro* and *in vivo* experiments. The transformation of ^{177}Lu to ^{177}Hf is accompanied by emission of gamma rays of 113 keV (3%) and 210 keV (11%) which are suitable for SPECT imaging. To verify the SPECT imaging capacity of the ^{177}Lu-microspheres, tube phantom imaging was carried out. The results given in Fig. 1F and Fig. S2 (Supporting information) reveal that the signal in-

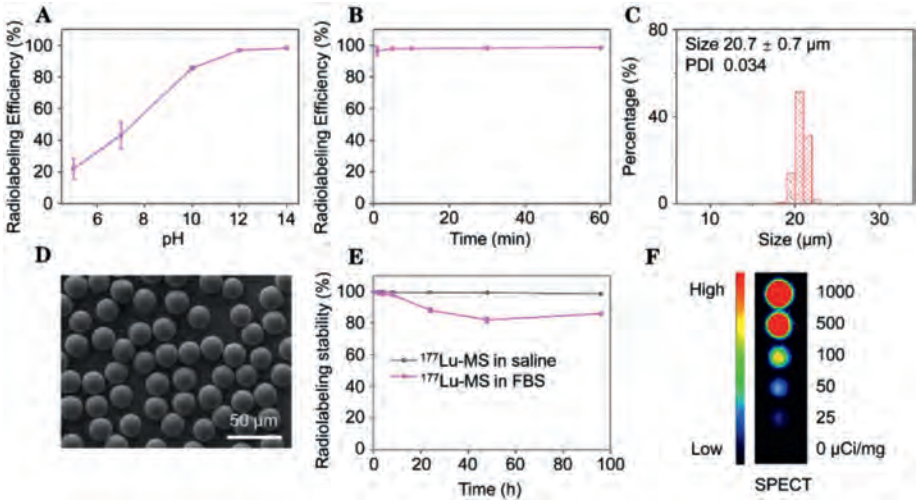

Fig. 1. (A) Radiolabeling efficiency as a function of pH. (B) Radiolabeling efficiency as a function of reaction time. (C-D) Histogram and SEM image of Lu-microspheres. (E) Radiostability of ^{177}Lu-microspheres in saline and 10% FBS. (F) Tube phantom image of ^{177}Lu-microsphere suspensions with radioactivity varying from 0 to 1000 μCi/mg.

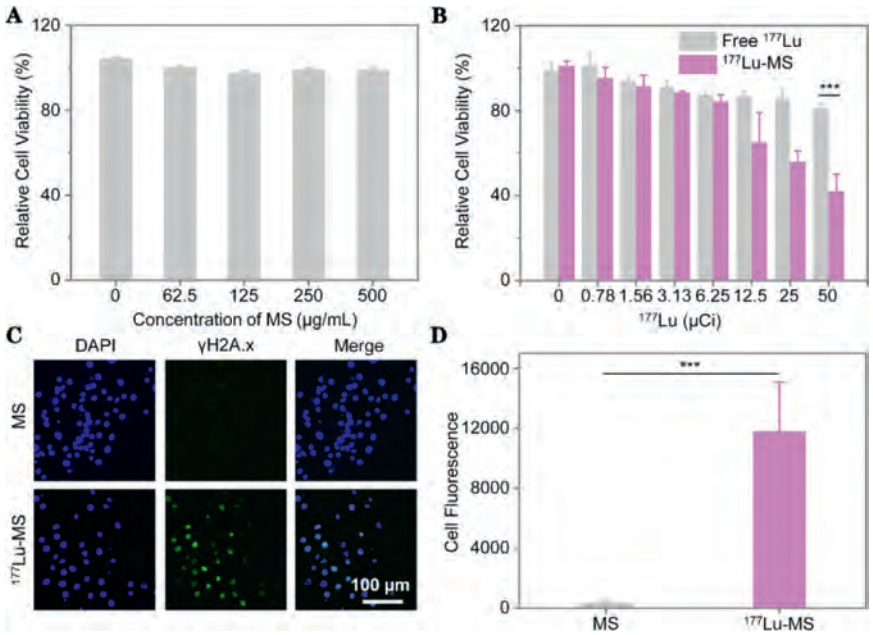

Fig. 2. (A) Relative viability of HepG2 cells incubated with silica microspheres (MS) at different concentrations. (B) Relative viability of HepG2 cells incubated with $^{177}LuCl_3$ and ^{177}Lu-microspheres with radioactivity varying from 0 to 50 μCi for 24 h (C) Immunofluorescence assays of HepG2 cells incubated with MS (0.5 mg/mL) and ^{177}Lu-microspheres (0.5 mg/mL, 200 μCi/mL), respectively. (D) Quantification of the immunofluorescence signal. *P* values were calculated by One-way ANOVA with Tukey multiple comparison tests, *** $P < 0.001$.

tensity extracted from SPECT images increases linearly against the radioactivity of ^{177}Lu-microspheres, suggesting that the ^{177}Lu-microspheres are potentially suitable for SPECT imaging of tumors *in vivo*. Most importantly, the SPECT signal offers a non-invasive way to track the ^{177}Lu-microspheres *in vivo*.

Before the *in vivo* study, the potential cytotoxicity of the mother silica microspheres and ^{177}Lu-microspheres to HepG2 liver cancer cells was evaluated by MTT assay. According to the results given in Fig. 2A, no obvious cytotoxicity was observed even at silica microspheres concentration of 500 μg/mL. However, at the same concentration of silica microspheres, 50 μCi radioactivity can induce significant cytotoxicity to HepG2, *e.g.*, the cell viability is decreased to 42.01% ± 8.02%, as shown in Fig. 2B. Those results could be explained by more energy deposited on cells, due to ^{177}Lu-microspheres close to the cells. In addition, the cytotoxicity of silica microspheres in normal cells was further tested. No obvious cytotoxicity was observed even at silica microspheres concentration of 500 μg/mL in 3T3 mouse embryonic fibroblast cells as shown in Fig. S3 (Supporting information).

The emission of electron of 490 keV during the transformation of ^{177}Lu to ^{177}Hf can induce DNA damage [39]. To evaluate this effect, an immunofluorescence assay was carried out to analyze the DNA damage. It was confirmed that ^{177}Lu-microspheres give rise to obvious DNA breakages contrasting to the mother silica microspheres (Fig. 2C). Further quantifying the immunofluorescence imaging results reveals that the fluorescence intensity induced by ^{177}Lu-microspheres is increased by a factor of 31 in comparison with that induced by silica microspheres, indicating that ^{177}Lu-microspheres possess a remarkable potential for treating HepG2 liver cancer (Fig. 2D).

The *in vivo* embolization of ^{177}Lu-microspheres was evaluated through a rabbit ear model. After 8 d embolization, the tip of rabbit right ear was avascular necrosis due to the obstruction of blood flow as shown in Fig. S4 (Supporting information), indicating that ^{177}Lu-microspheres could achieve good embolization.

Prior to the anti-tumor treatment, the imaging performance of ^{177}Lu-microspheres was evaluated on HepG2 cell tumor-bearing BALb/c nude mice by using free $^{177}Lu^{3+}$ as control. After intratumoral injection, SPECT scans were conducted at different time points postinjection. It can be observed that the signal of ^{177}Lu-microspheres remains visualizable for 32 d postinjection (Fig. 3A). More importantly, no radioactivity was found in other organs or tissues, suggesting that ^{177}Lu-microspheres were very stable *in vivo*. According to the quantification analysis of the SPECT images, the radioactivity of ^{177}Lu-microspheres in tumor decreases against time, perfectly consistent with the theoretical physical half-life attenuation of ^{177}Lu (Fig. 3B), supporting that the ^{177}Lu-microspheres in the tumor do not release the ^{177}Lu payload to other organs. In contrast, free ^{177}Lu gives rise to visualizable signal only for 12 d postinjection, due to the complexation between $^{177}Lu^{3+}$ and protein [40]. On the one hand, the tumor became too big (1500 mm^3) after that to allow the continuation of the experiment and on the other hand ^{177}Lu was found to diffuse obviously from the tumor site to whole body and accumulate particularly in bone. In consequence, the radiation dose is dramatically decreased as shown in Fig. 3B.

To accurately trace the distribution of ^{177}Lu, the radioactivity of organs and tissues extracted after the imaging study were measured by γ counter. The results given in Fig. 3C confirm that almost no ^{177}Lu ion is released by ^{177}Lu-microspheres, while apart from tumor (3.1% ± 0.6% ID/g), radioactivity of ^{177}Lu can also be detected from other organs and tissues such as bone (2.8% ± 0.05% ID/g) if ^{177}Lu is delivered in the form of $LuCl_3$. It was also observed that it took just a few hours for bone to show evident signal postadministration of free ^{177}Lu (Fig. S5 in Supporting information), eventually leading to significant signal at the end. This is because as a lanthanide element lutetium has a strong osteophilicity in the body. All these results suggest that ^{177}Lu-microspheres hold a great potential as a radiopharmaceutical for liver cancer treatment.

The tumor-therapeutic effect of the ^{177}Lu-microspheres was evaluated through tumor inhibition experiments on HepG2 cell tumor-bearing BALb/c nude mice. The tumor-bearing mice were randomly divided into four groups and received saline, mother silica microspheres, ^{177}Lu-microspheres with different doses, *i.e.*,

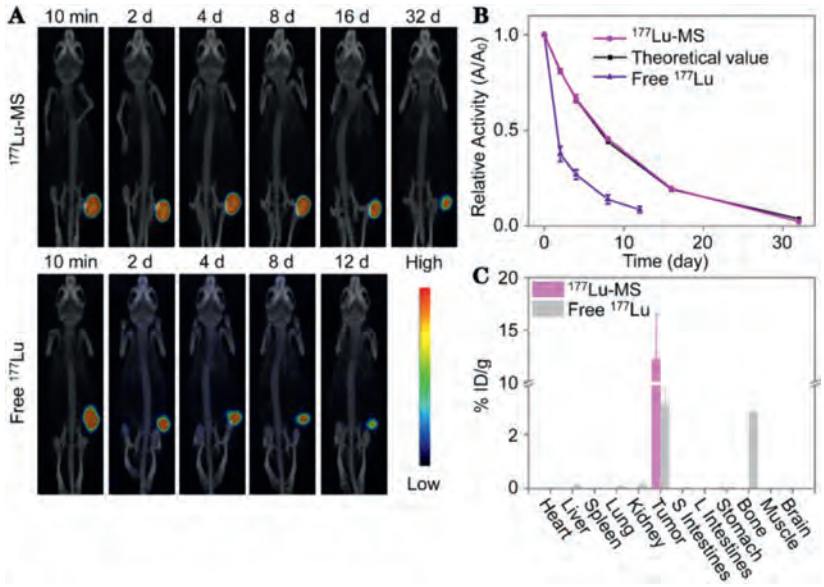

Fig. 3. (A) SPECT/CT images of HepG2 tumor-bearing mice intratumorally injected with ^{177}Lu-microspheres (1 mCi) (denoted as ^{177}Lu-MS) and $^{177}LuCl_3$ (100 μCi) (denoted as Free ^{177}Lu). (B) Relative temporal activity of the tumorous regions overlaid with a theoretical decay curve for ^{177}Lu. (C) Biodistribution of ^{177}Lu obtained 12 d and 32 d after the delivery in the form of $^{177}LuCl_3$ and ^{177}Lu-microspheres, respectively.

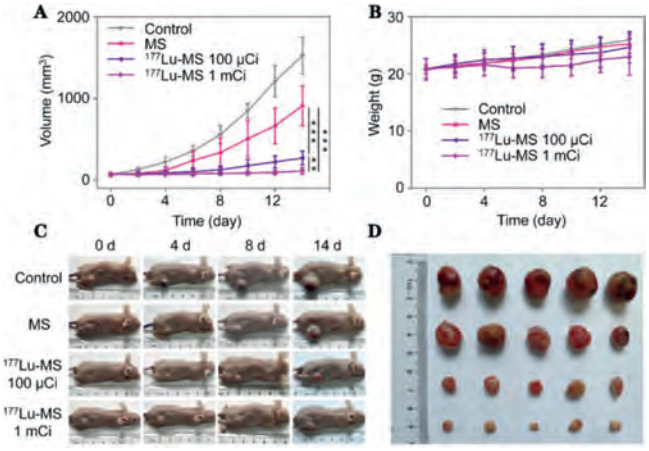

Fig. 4. (A, B) Tumor volume and body weight of HepG2 tumor-bearing mice treated with saline (control), MS (50 mg/kg), ^{177}Lu-microspheres with different radioactivity (*i.e.*, 100 μCi and 1 mCi), respectively. (C) Photographs of representative HepG2 tumor-bearing mice recorded during the treatment. (D) Photograph of tumors extracted 14 d post-treatment. *P* values were calculated by One-way ANOVA with Tukey multiple comparison tests, $^{**}P < 0.01$, $^{***}P < 0.001$.

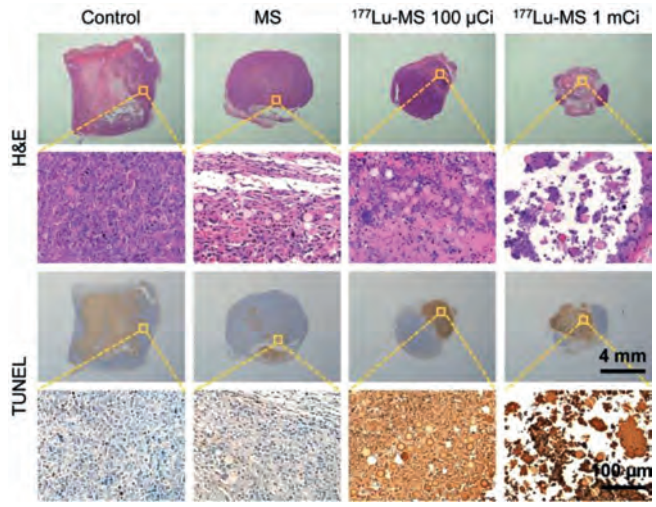

Fig. 5. Macroscopic images of HepG2 tumor slices obtained 14 d post-treatment and stained with H&E and TUNEL, respectively.

100 μCi and 1 mCi, respectively. The cumulative tumor radiation of 1 mCi and 0.1 mCi groups amounted to 551.3 Gy/g and 55.1 Gy/g, respectively, within the first 14 d postinjection. Notably, the ^{177}Lu-microspheres can significantly inhibit the tumor growth (Fig. 4A), particularly the 1 mCi group. Although the tumors of the 1 mCi treatment group didn't completely vanish, a better treatment efficacy can still be expected because radioembolization will surely give rise to a better distribution of than ^{177}Lu-microspheres than that achieved by intratumoral administration.

The volumes of the tumors were recorded every 2 days with a vernier caliper, and the body weights were also monitored. As shown in Fig. 4B, the treatment with ^{177}Lu-microspheres does not lead to obvious loss of body weight compared to other reference groups, demonstrating that the ^{177}Lu-microspheres have no obvious side effects. The photos of representative mice from each group are shown in Fig. 4C.

The physiological conditions of the mice look very good. As the tumor volume of control group reached 1500 mm^3, the mice were sacrificed according to ethical rules. The tumors collected from different groups are shown in Fig. 4D for comparison.

The tumor and main organs including heart, liver, spleen, lung, and kidney of the mice receiving different treatments were sliced and then subjected to hematoxylin and eosin (H&E) and TUNEL staining. As shown in Fig. 5, the treatment with ^{177}Lu-microspheres can apparently give rise to remarkable necrosis and apoptosis in comparison with the control group and silica microspheres group. More importantly, the H&E staining reveals that nearly no damage was created by the ^{177}Lu-microspheres groups to major organs as given in Fig. 6.

In summary, we have developed a facile and effective approach for preparing ^{177}Lu-microspheres capable of inhibiting the tumor growth apart from being visualizable with SPECT. Through sim-

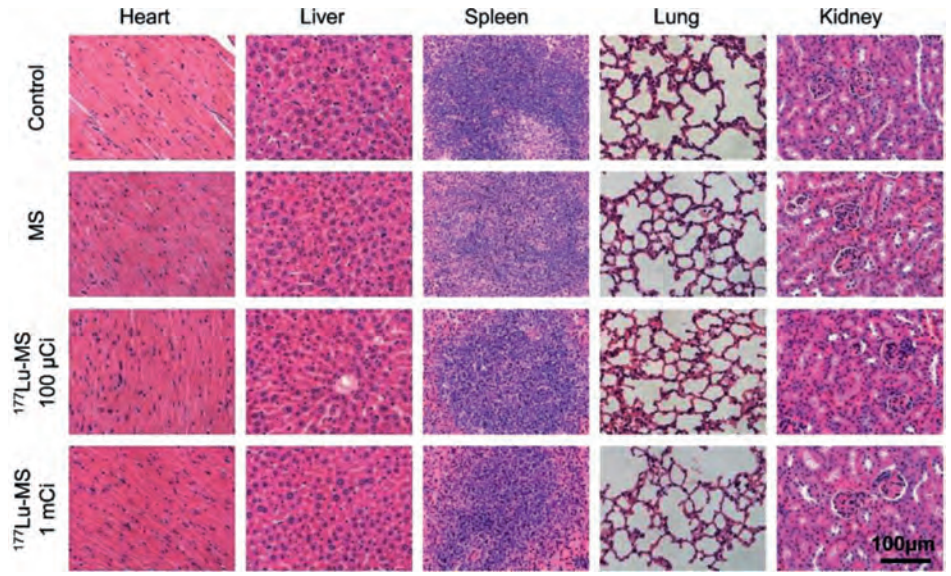

Fig. 6. Macroscopic H&E staining images of different organs of HepG2 tumor-bearing mice harvested 14 d post-treatment.

ple precipitation method, the radiolabeling efficiency as high as 96.8% ± 0.5% has been successfully achieved and the specific activity of the resulting ^{177}Lu-microspheres with outstanding radiostability can be controlled over a broad range from 1 Bq to 1 × 10^5 Bq/microsphere. Over 30-day observation demonstrates that the ^{177}Lu labeling is super robust *in vivo*. The tumor therapeutic studies reveal that the ^{177}Lu-microspheres can effectively inhibit the growth of HCC, demonstrated on the subcutaneous mice tumor model, and induce no obvious side effects. Therefore, ^{177}Lu-microspheres hold great potential as radioembolic microspheres for precise radioisotope therapy of HCC.

Ethical statement

All animal experiments were approved by the Animal Care and Use Committee of Soochow University, and all protocols of animal studies conformed to the Guide for the Care and Use of Laboratory Animals of Soochow University, China.

Declaration of competing interest

The authors declare no competing financial interest.

Acknowledgments

The authors thank the financial support from the National Natural Science Found of China (Nos. 81720108024, 21976128), Priority Academic Program Development of Jiangsu Higher Education Institutions (PAPD). G. Wang thanks the support from the Natural Science Foundation of Jiangsu Province (No. BK20200100).

Supplementary materials

Supplementary material associated with this article can be found, in the online version, at doi:10.1016/j.cclet.2022.01.007.

References

[1] H. Sung, J. Ferlay, R.L. Siegel, et al., CA-Cancer J. Clin. 71 (2021) 209–249.
[2] J.D. Yang, P. Hainaut, G.J. Gores, et al., Nat. Rev. Gastroenterol. Hepatol. 16 (2019) 589–604.
[3] E. Vibert, M. Schwartz, K.M. Olthoff, J. Hepatol. 72 (2020) 262–276.
[4] S. Lee, T.W. Kang, K.D. Song, et al., Ann. Surg. 273 (2021) 564–571.
[5] N. Kim, J. Cheng, I. Jung, et al., J. Hepatol. 73 (2020) 121–129.
[6] R.S. Finn, A.X. Zhu, W. Farah, et al., Hepatology 67 (2018) 422–435.
[7] S. Daher, M. Massarwa, A.A. Benson, T. Khoury, J. Clin. Transl. Hepatol. 6 (2018) 69–78.
[8] J. Edeline, Y. Touchefeu, B. Guiu, JAMA Oncol. 6 (2020) 51–59.
[9] M. Kudo, K. Ueshima, M. Ikeda, et al., Gut 69 (2020) 1492–1501.
[10] J.L. Raoul, A. Forner, L. Bolondi, et al., Cancer Treat. Rev. 72 (2019) 28–36.
[11] E. Lanza, M. Donadon, D. Poretti, et al., Liver Cancer 6 (2017) 27–33.
[12] B. Toskich, T. Patel, Hepatology 67 (2018) 820–822.
[13] H.-.C. Kim, Clin. Mol. Hepatol. 23 (2017) 109–114.
[14] N. Venkatanarasimha, A. Gogna, K.T.A. Tong, et al., Clin. Radiol. 72 (2017) 1002–1013.
[15] A. Laurent, Tech. Vasc. Interv. Radiol. 10 (2007) 248–256.
[16] P. d'Abadie, M. Hesse, A. Louppe, et al., Molecules 26 (2021) 3966–3979.
[17] C.A. Arnold, M.K. Pezhouh, D. Lam-Himlin, et al., Am. J. Surg. Pathol. 43 (2019) 688–694.
[18] M.A. Westcott, D.M. Coldwell, D.M. Liu, J.F. Zikria, et al., Adv. Radiat. Oncol. 1 (2016) 351–364.
[19] L. Filippi, O. Schillaci, O. Bagni, Eur. J. Nucl. Med. Mol. Imaging 45 (2018) 2238–2239.
[20] M.T.M. Reinders, M.L.J. Smits, C. van Roekel, A. Braat, Semin. Nucl. Med. 49 (2019) 237–243.
[21] J.F. Prince, R. van Rooij, G.H. Bol, et al., J. Nucl. Med. 56 (2015) 817–823.
[22] F. Pang, Y. Li, W. Zhang, et al., Adv. Healthc. Mater. 9 (2020) e2000028.
[23] Y. Qian, Q. Liu, P. Li, et al., ACS Nano 15 (2021) 2933–2946.
[24] Q.F. Liu, Y.Y. Qian, P. Li, et al., Theranostics 8 (2018) 785–799.
[25] L.C. Chen, Y.J. Chang, S.J. Chen, et al., Int. J. Radiat. Biol. 93 (2017) 477–486.
[26] J.C. De La Vega, P.L. Esquinas, C. Rodriguez-Rodriguez, et al., Theranostics 9 (2019) 868–883.
[27] H.C. Ni, C.Y. Yu, S.J. Chen, et al., Appl. Radiat. Isot. 99 (2015) 117–121.
[28] P.F. Chiang, C.L. Peng, Y.H. Shih, et al., ACS Biomater. Sci. Eng. 4 (2018) 3425–3433.
[29] D. Cvjetinovic, Z. Prijovic, D. Jankovic, et al., J. Control. Release 332 (2021) 301–311.
[30] U. Pandey, S. Subramanian, S. Shaikh, et al., Radiopharm 34 (2019) 306–315.
[31] K. Rahbar, A. Bode, M. Weckesser, et al., Clin. Nucl. Med. 41 (2016) 522–528.
[32] C. Kratochwil, F.L. Giesel, M. Stefanova, et al., J. Nucl. Med. 57 (2016) 1170–1176.
[33] M. Benesova, M. Schafer, U. Bauder-Wust, et al., J. Nucl. Med. 56 (2015) 914–920.
[34] H.B. Sayman, F. Gulsen, S. Sager, et al., J. Vasc. Interv. Radiol. (2021), doi:10.1016/j.jvir.2021.10.016.
[35] M.H. Ju, Y.P. Li, L. Yu, C.Q. Wang, L.X. Zhang, Microporous Mesoporous Mat. 247 (2017) 75–85.
[36] A. Dohare, S. Sudhakar, B. Brodbeck, et al., Langmuir 37 (2021) 13460–13470.
[37] K. Sato, R.J. Lewandowski, J.T. Bui, et al., Cardiovasc. Interv. Radiol. 29 (2006) 522–529.
[38] P.M. Piana, V. Bar, L. Doyle, et al., HPB 16 (2014) 336–341.
[39] E. O'Neill, V. Kersemans, P.D. Allen, et al., J. Nucl. Med. 61 (2020) 743–750.
[40] T. Dudev, C. Lim, Chem. Rev. 114 (2014) 538–556.